Original

Lv, J.; Yang, J.; Hao, X.; Ren, X.; Feng, Y.; Zhang, W.:

Biodegradable PEI modified complex micelles as gene carriers with tunable gene transfection efficiency for ECs

In: Journal of Materials Chemistry B (2016) Royal Society of Chemistry

DOI: 10.1039/c5tb02310f

Journal of
Materials Chemistry B

PAPER

View Article Online
View Journal | View Issue

Cite this: J. Mater. Chem. B, 2016, 4, 997

Biodegradable PEI modified complex micelles as gene carriers with tunable gene transfection efficiency for ECs

Juan Lv,†[ab] Jing Yang,†[ab] Xuefang Hao,[ab] Xiangkui Ren,*[a] Yakai Feng*[abcd] and Wencheng Zhang*[e]

Received 5th November 2015,
Accepted 20th December 2015

DOI: 10.1039/c5tb02310f

www.rsc.org/MaterialsB

In recent years, gene therapy has evoked an increasing interest in clinical treatments of coronary diseases because it is a potential strategy to realize rapid endothelialization of artificial vascular grafts. The balance of high transfection efficiency and low cytotoxicity of nonviral gene carriers is an important issue to be solved. In this study, we aim to establish a gene delivery system offering an elegant way to tune the transfection activity and cytotoxicity. Biodegradable complex micelles were prepared from polyethylenimine-*b*-poly(lactide-*co*-3(*S*)-methyl-morpholine-2,5-dione)-*b*-polyethylenimine (PEI-*b*-PLMD-*b*-PEI) and methoxy-poly(ethylene glycol)-*b*-poly(lactide-*co*-3(*S*)-methyl-morpholine-2,5-dione) (mPEG-*b*-PLMD) copolymers by a co-assembly method. Then the ZNF580 gene plasmid (pDNA) was encapsulated into the complex micelles. The hydrodynamic size and zeta potential of these complex micelles and micelles/pDNA complexes indicated that they were feasible for use in cellular uptake and gene transfection. As expected, the transfection efficiency and cytotoxicity of these micelles/pDNA complexes could be conveniently tuned by changing the mass ratio of mPEG-*b*-PLMD to PEI-*b*-PLMD-*b*-PEI (3/1, 2/2, 1/3 and 0/4) in the mixed mPEG/PEI shell. The transfection efficiency increased as the mass ratio of mPEG-*b*-PLMD/PEI-*b*-PLMD-*b*-PEI decreased from 3/1 to 0/4, while the cytotoxicity showed an opposite tendency. Moreover, ZNF580 protein expression determined by Western blot analysis and the migration of transfected endothelial cells (ECs) by wound healing assay were consistent with the result of transfection efficiency. All these results indicated that the co-assembled complex micelles could act as suitable gene carriers with tunable gene transfection efficiency and cytotoxicity, which should have great potential for the transfection of vascular ECs.

1. Introduction

Rapid *in situ* endothelialization is a crucial first step to prevent the formation of thrombosis and neointimal hyperplasia of vascular prostheses after cardiovascular treatments.[1] Nowadays, gene therapy plays a crucial role in the rapid endothelialization of artificial vascular grafts.[2] The transfection of genes into endothelial cells (ECs) has been reported as an efficient method to create an endothelial layer over the surface of scaffolds.[3] Vascular endothelial growth factor (VEGF) is a widely used growth factor to promote angiogenesis and to enhance revascularisation and re-endothelialization.[4] Besides VEGF, the ZNF580 gene as a human C_2H_2-zinc finger protein gene can promote the expression of VEGF to enhance the proliferation and migration of ECs.[5–8] Furthermore, compared with VEGF, the ZNF580 gene can inhibit the proliferation of smooth muscle cells (SMCs). It is beneficial for addressing the competitive growth of SMCs over ECs; otherwise the overgrowth of SMCs might lead to failure of formation of a complete endothelium.

The gene transfection efficiency and cytotoxicity of gene delivery systems usually depend on gene carriers.[9] In recent years, nonviral carriers have been considered as an attractive alternative to viral carriers in gene delivery systems for their relative safety and low pathogenic and immunogenic properties.[10–23] Among various kinds of nonviral gene carrier materials, polyethylenimine (PEI), offering the gold standard of gene transfection, is one of the most successful cationic polymers for gene delivery both *in vitro* and *in vivo*.[9,10] However, high molecular weight PEI is reported to be cytotoxic due to its high cationic

[a] School of Chemical Engineering and Technology, Tianjin University, Weijin Road 92, Tianjin 300072, China. E-mail: yakaifeng@tju.edu.cn
[b] Collaborative Innovation Center of Chemical Science and Chemical Engineering (Tianjin), Weijin Road 92, Tianjin 300072, China
[c] Key Laboratory of Systems Bioengineering of Ministry of Education, Tianjin University, Weijin Road 92, Tianjin 300072, China
[d] Tianjin University-Helmholtz-Zentrum Geesthacht, Joint Laboratory for Biomaterials and Regenerative Medicine, Weijin Road 92, Tianjin 300072, China
[e] Department of Physiology and Pathophysiology, Logistics University of Chinese People's Armed Police Force, Tianjin 300162, China
† Juan Lv and Jing Yang contributed equally to this work.

charge density[24] and could cause self-aggregation and adherence on the cell surface, which results in significant necrosis.[25] Thus low or no cytotoxicity should be taken into account in the design of novel gene delivery systems for practical application. For this purpose, one of the most extensively investigated attempts to shield the cationic charge of PEI is to introduce the neutral hydrophilic poly(ethylene glycol) (PEG) into gene delivery systems. By virtue of the properties of hydrophilicity and electrical neutrality and the ability to counteract protein absorption,[26–29] the PEG block can indeed reduce the cytotoxicity and prolong the circulation time of these nanocarriers,[30,31] but at the same time may interfere with DNA complexation, leading to poor transfection efficiency.[23,32]

Polymeric micelles have been developed by self-assembly of amphiphilic block copolymers and used especially in drug and gene delivery systems.[33,34] In our previous studies, we have prepared several biodegradable gene carriers by self-assembly of triblock amphiphilic copolymers,[6,7,35,36] whereby the proliferation and migration of ECs were significantly improved by the delivery of the ZNF580 gene using these carriers. It should be noted, nevertheless, that the synthesis of these triblock copolymers requires rigorous reactive conditions and complicated multi-step processes; furthermore the mass ratio of PEI and PEG in gene carriers is difficult to precisely control. Thus it is necessary to simplify the reactive conditions and synthetic processes of the triblock copolymers for gene carriers. In parallel with the efforts to obtain multifunctional polymers for self-assembly through complicated polymerization techniques, an alternative strategy of cooperative self-assembly of several block polymers into complex polymeric micelles offers a convenient preparation process of multifunctional gene carriers.[37] This strategy provides us an elegant way to tune various physical properties and biological functions of carriers easily *via* changing the ratios of different shell-forming block copolymers.[38,39] It is of great interest to know whether it is possible to prepare gene carrier systems with tunable gene transfection efficiency for ECs by cooperative self-assembly of several block copolymers.

The purpose of the present study is to develop a gene delivery system with the simplicity of tuning transfection efficiency and cytotoxicity simultaneously by co-assembly of two kinds of biodegradable polymers. PEI (M_w = 10 kDa) was used for grafting onto the biodegradable poly(lactide-*co*-3(*S*)-methyl-morpholine-2,5-dione) (PLMD) backbone. 3(*S*)-Methyl-morpholine-2,5-dione (MMD) is a kind of monomer of cyclodepsipeptides, which have been used to synthesize biodegradable polydepsipeptides as drug or gene delivery matrices with alternating amido and ester groups.[40–43] The hydrolysis of polydepsipeptide segments produces L-amino acids that buffer the pH of the degradation microenvironment. Thus, it could reduce the inflammation resulting from the acidic environment. Moreover, the degradation products including L-amino acids can be properly metabolized by living tissues.[44,45] In addition, this gene carrier with a hydrophobic PLMD core could enhance the stabilization of micelles compared with polyplexes assembled from homo-PEI or PEG-*b*-PEI and DNA.[46,47] The co-micellization of the PEI modified copolymer (PEI-*b*-PLMD-*b*-PEI) and methoxy-poly(ethylene glycol)-*b*-poly(lactide-*co*-3(*S*)-methyl-morpholine-2,5-dione) (mPEG-*b*-PLMD) could form a complex micelle with a biodegradable PLMD core and a mixed mPEG/PEI shell of different mass ratios (Scheme 1). Then, the ZNF580 gene plasmid (plasmid fused to green fluorescent protein, pEGFP-ZNF580, pDNA), which has the ability of enhancing the transfection of vascular ECs, was condensed with PEI located at the interface between the PLMD core and the mPEG shell. The properties of the complex micelles and micelles/pDNA complexes were characterized by diffraction light scattering. Furthermore, the trends of transfection efficiency and cytotoxicity of these micelles/pDNA complexes were investigated by simply changing the mass ratio of mPEG to PEI in the mixed shell. Moreover, Western blot analysis and wound healing assay were also performed to confirm the transfection efficiency and migration ability of the transfected ECs. Our study developed a simple way to tune the transfection efficiency and cytotoxicity of gene carriers, which can provide a convenient method to explore novel gene delivery systems.

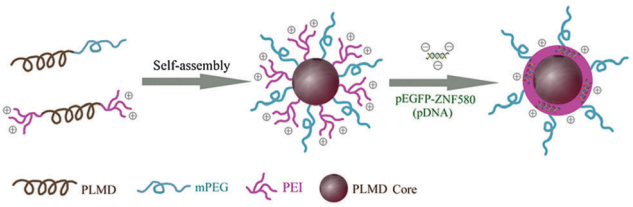

Scheme 1 Self-assembly of complex micelles and condensation of pDNA.

2. Materials and methods

2.1. Materials

L-Alanine (food grade) and chloroacetyl chloride were supplied by Aladdin Reagent Co., Ltd (Shanghai, China). Poly(ethylene glycol) monomethyl ether (mPEG, M_w = 5 kDa and polydispersity index (PDI) = 1.05) was purchased from Aldrich and dried in vacuum for 24 h before use. Polyethylenimine (branched PEI, M_w = 10 kDa), 4-dimethylamino pyridine (DMAP), *N*-hydroxy succinimide (NHS), 1-ethyl-3-(3-dimethylaminopropyl)-carbodiimide hydrochloride (EDC) and stannous octoate ($Sn(Oct)_2$) were purchased from Sigma-Aldrich (Beijing, China) and used without further purification. L-Lactide (LLA) was obtained from Foryou Medical Device Co., Ltd (Huizhou, China). 1,8-Octanediol, succinic anhydride, triethylamine (Et_3N), 1,4-dioxane and toluene were purchased from the Institute of Guangfu Fine Chemical Research (Tianjin, China) and they were dried by refluxing over CaH_2 and distilled just before use.

The BCA protein assay kit was purchased from Solarbio Science and Technology Co., Ltd (Beijing, China). 3-(4,5-Dimethylthiazol-2-yl)-2,5-diphenyltetrazolium bromide (MTT), rabbit anti-human ZNF580 polyclonal antibody and goat anti-rabbit IgG were purchased from Abcam (HK) Ltd (Hong Kong, China). The pDNA was preserved by the Department of Physiology and Pathophysiology, Logistics University of Chinese People's Armed Police Force. Other chemicals were analytically pure and purchased from Jiangtian Chemicals (Tianjin, China).

2.2. Synthesis of the mPEG-*b*-PLMD block copolymer

MMD was synthesized according to the literature.[48] The crude product was recrystallized from absolute acetonitrile to obtain colorless crystals with 43% yield, m.p. 139–142 °C. The mPEG-*b*-PLMD block copolymer was synthesized by ring-opening polymerization (ROP) of MMD and LLA initiated by the hydroxyl group of mPEG with $Sn(Oct)_2$ as a catalyst. Typically, 2.0 g (0.40 mmol) of mPEG was introduced into a Schlenk tube under a nitrogen atmosphere. Then 0.40 g (3.1 mmol) of MMD, 3.4 g (23.7 mmol) of LLA, and 400 μL of 0.25 mol L^{-1} $Sn(Oct)_2$ solution in dry toluene were added successively, and submitted to vacuum/nitrogen cycles. The Schlenk tube was finally sealed under dry nitrogen and reacted at 150 °C for 24 h. Then the polymer was dissolved in chloroform and precipitated from *n*-hexane/chloroform (6/1; v/v) for three times, and dried at room temperature for 24 h under vacuum. The yield was 86.5%.

2.3. Synthesis of the PEI-*b*-PLMD-*b*-PEI block copolymer

2.3.1. Synthesis of the PLMD polymer. PLMD was synthesized by ROP of MMD and LLA using 1,8-octanediol as an initiator and $Sn(Oct)_2$ as a catalyst. Briefly, 0.070 g (0.50 mmol) of 1,8-octanediol, 0.50 g (3.8 mmol) of MMD and 4.50 g (31.3 mmol) of LLA were weighed into a Schlenk tube equipped with a magnetic stirring bar and submitted to vacuum/nitrogen cycles. The Schlenk tube was sealed and maintained at 150 °C for 24 h. The product was purified by precipitating into *n*-hexane/chloroform (6/1; v/v) from chloroform solution (repeated three times) and dried at room temperature for 24 h under vacuum. The yield was 91.1%.

2.3.2. Synthesis of HOOC-PLMD-COOH. Carboxyl-terminated PLMD (HOOC-PLMD-COOH) was synthesized as previously reported.[49] Briefly, PLMD (3.10 g, 0.3 mmol), succinic anhydride (0.60 g, 6.1 mmol), Et_3N (250 μL) and DMAP (0.80 g, 6.1 mmol) were dissolved into 25 mL of dry 1,4-dioxane in a round bottom flask. The reaction was performed at 25 °C under a dry nitrogen atmosphere for 24 h. The crude product was obtained by precipitation into cold ethanol and then it was redissolved in chloroform followed by washing with hydrochloric acid aqueous solution (10% in v/v), saturated sodium bicarbonate solution, and saturated sodium chloride solution; each step was repeated three times. The aqueous phase was abandoned and the organic phase was dried over anhydrous sodium sulphate. The final product of HOOC-PLMD-COOH was obtained by precipitating into cold *n*-hexane and dried under vacuum at room temperature for 24 h (yield: 66.1%).

2.3.3. Synthesis of the PEI-*b*-PLMD-*b*-PEI block copolymer. HOOC-PLMD-COOH (0.50 g, 0.05 mmol), EDC (0.10 g, 0.5 mmol), and NHS (0.06 g, 0.5 mmol) were first dissolved in 10 mL of DMSO and reacted at room temperature for 1 h, and then PEI (1.10 g, 0.10 mmol in 2 mL of DMSO) was added. The reaction was continued at room temperature with stirring for 24 h, and then the whole solution was dialyzed (MWCO = 14 kDa) against distilled water for 2 days to remove the organic solvent and unreacted stuff. Finally, the product in the dialysis bag was lyophilized to obtain the triblock copolymer PEI-*b*-PLMD-*b*-PEI (yield: 64.2%).

2.4. Characterization of block copolymers

^1H nuclear magnetic resonance (^1H NMR) spectroscopy was used to characterize the polymer structures on an ECA-500 400 MHz spectrometer in deuterochloroform ($CDCl_3$) at 25 °C. Gel permeation chromatography (GPC) was performed to measure the number-average molecular weight (M_n), weight-average molecular weight (M_w) and PDI at 25 °C using a Waters 1525 chromatograph equipped with a Waters 2414 refractive index detector. *N*,*N*-Dimethylformamide (DMF) was used as the eluent at a flow rate of 1.0 mL min^{-1} and polystyrene as a standard.

2.5. Preparation of complex micelles with varying ratios of mPEG to PEI

The block copolymers of mPEG-*b*-PLMD and PEI-*b*-PLMD-*b*-PEI were separately dissolved in DMF to obtain two polymer solutions with a concentration of 5.0 mg mL^{-1}, respectively. Subsequently, different volumes of the two solutions were mixed to prepare a series of solutions with different mass ratios of mPEG-*b*-PLMD and PEI-*b*-PLMD-*b*-PEI (3/1, 2/2, 1/3, and 0/4, respectively). Then 2.0 mL of the mixed polymer solution was dropped into 10 mL of phosphate buffer solution (PBS, pH = 7.4) and dialyzed against PBS for 2 days (MWCO = 3.5 kDa) to obtain the complex micelle solution (0.75 mg mL^{-1}).

2.6. Formation of the micelles/pDNA complexes

pDNA solution (0.10 mg mL^{-1}) was added dropwise into micelle solutions under stirring to prepare micelles/pDNA complexes at different N/P molar ratios (1, 3, 5, 10, 15 and 20). The complexes were incubated for 0.5 h before characterization and further use.

2.7. Physicochemical characterization of complex micelles and micelles/pDNA complexes

The hydrodynamic size and structures of the complex micelles and micelles/pDNA complexes were characterized by a combination of dynamic light scattering (DLS) and static light scattering (SLS) measurements. DLS and SLS measurements were performed at 636 nm by using a laser light scattering spectrometer (BI-200SM) equipped with a digital correlator (BI-9000AT). The zeta potential of complex micelles and micelles/pDNA complexes was measured using a DLS (Malvern Zetasizer NanoZS4700) instrument operating with vertically polarized light from a 633 nm argon-ion laser.

2.8. Biological characterization of micelles/pDNA complexes

2.8.1. Cell line and cell culture. The human endothelial cell hybridoma line EA.hy926 purchased from American Type Culture Collection was cultured in high-glucose DMEM supplemented with 10% FBS in an incubator at 37 °C with 5% CO_2. The cells were cultured to confluence with medium exchanges every other day.

2.8.2. Agarose gel electrophoresis. Agarose gel electrophoresis was performed to assess the pDNA condensation ability of complex micelles. The micelles/pDNA complexes with N/P molar ratios ranging from 0 to 15 were prepared. Then they were loaded onto

the agarose gel (0.8%) containing 0.5 μg mL^{-1} ethidium bromide in 1 × TAE buffer and electrophoresed at 100 V for 30 min. A UV illuminator was used to indicate the retarded location of the pDNA.

2.8.3. MTT assay. The cytotoxicity of complex micelles and micelles/pDNA complexes was evaluated by MTT assay. Briefly, EA.hy926 cells were firstly seeded in a 96-well plate (1×10^4 cells per well) and cultured for 24 h until they reached 50–60% confluence. Next, the cells were starved in serum-free medium for 12 h. Micelles and micelles/pDNA complexes with different micelle concentrations at a N/P molar ratio of 15 were prepared and added into the cells in fresh growth medium containing 10% FBS. PEI 10 kDa was used as a control group. After 24 h, 20 μL of MTT solution (5 mg mL^{-1}) was added into each well for another 4 h. Then, the medium was removed carefully and 150 μL of dimethylsulfoxide was added to each well to dissolve the formed formazan crystals. The 96-well plate was oscillated at low speed on a volatility instrument for 10 min, and optical density (OD) was measured using a microplate reader (Bio-Rad, IMARKTM) at a wavelength of 490 nm. The relative cell viability (%) was calculated using the following formula:

$$\text{Relative cell viability} = \frac{\text{OD490}'}{\text{avg(OD490C}')} \times 100\%$$

where OD490′ is the absorbance value of experimental wells minus zero wells and avg(OD490C′) is the average absorbance value of corrected control wells. At least three parallels were performed for each sample.

2.8.4. *In vitro* transfection of ECs. EA.hy926 cells were seeded in a 24-well plate at a density of 1×10^5 cells per well and cultured for 24 h until they reached 50–60% confluence. Before transfection, the cells were incubated with serum-free medium for 12 h. Micelles/pDNA complexes with a N/P molar ratio of 15 and a concentration of 30 μg mL^{-1} (1 μg pDNA per well) were added into each well. After 4 h, the medium was changed with fresh growth medium (10% FBS in DMEM). Then, the cells were further incubated to obtain considerable efficiency of gene transfection; the expression of green fluorescent protein (GFP) in cells was observed under an inverted fluorescent microscope at 12 h and 24 h.

2.8.5. Western blot assay. To determine the expression of ZNF580, Western blot analysis was performed as reported previously.[50] Cells were washed twice with 0.1 mol L^{-1} PBS (pH = 7.4) and then lysed in RIPA lysis buffer. The concentration of the lysate was determined using a BCA protein assay kit. Cell lysates containing 50 μg of protein were subjected to SDS-PAGE by using 15% polyacrylamide resolving gels. After electrophoresis, proteins were transferred onto polyvinylidene fluoride (PVDF) membranes. Proteins were first incubated with a rabbit anti-ZNF580 polyclonal antibody and then horseradish peroxidase conjugated goat anti-rabbit IgG to assess the protein loading level. Next, they were incubated with enhanced chemiluminescence reagent and exposed to the film. The belts were analyzed using Image J 2.1. β-Actin was used as a control.

2.8.6. Wound healing assay. The migration capability of EA.hy926 cells treated with micelles/pDNA complexes was assessed using the wound healing assay.[51] Briefly, EA.hy926 cells were transfected with micelles/pDNA complexes at the N/P molar ratio of 15. After 48 h, the transfected cells growing on 6-well dish plates to a 100% confluent monolayer were scratched to create a "wound" using a sterile 200 μL pipet tip. Cellular debris was removed by washing with D-Hanks buffer (pH = 7.4). The images were recorded at 0, 6 and 12 h after scratch formation using an inverted microscope; the migration area was calculated using Image J 2.1 based on the images after 12 h. The wounded area was calculated by the following formula: wounded area = length × width; the percentage of migration area was calculated by the following formula: migration area (%) = (wounded area − non-recovered area)/wounded area.[52]

2.9. Statistical analysis

Each experiment was repeated three times, and all data were expressed as the mean ± SD (standard deviation). Statistical analysis was performed using analysis of variance (ANOVA), and P values < 0.05 were considered statistically significant.

3. Results

3.1. Synthesis and characterization of mPEG-*b*-PLMD and PEI-*b*-PLMD-*b*-PEI copolymers

The synthetic routes toward mPEG-*b*-PLMD and PEI-*b*-PLMD-*b*-PEI copolymers are illustrated in Scheme 2. The amphiphilic copolymer of mPEG-*b*-PLMD was synthesized by ROP of LLA and MMD initiated by the hydroxyl group of mPEG with $Sn(Oct)_2$ as a catalyst. The M_n of mPEG-*b*-PLMD was confirmed by ^1H NMR analysis through the calculation of the integral intensity at 3.65 ppm (CH_2CH_2O in mPEG), 5.18 ppm ($OCHCH_3CO$ in LLA residue), and 4.70 ppm ($COCHCH_3NH$ in MMD residue) based on the known molecular weight of mPEG. The M_n of mPEG-*b*-PLMD was calculated to be 15 kDa, and the content of LLA in the PLMD block was 84.2% calculated from the integral area of the peaks mentioned above. The amphiphilic copolymer of PEI-*b*-PLMD-*b*-PEI was synthesized through three steps. Firstly, the dihydroxyl copolymer HO-PLMD-OH was synthesized by ROP of LLA and MMD using 1,8-octanediol as an initiator. The obtained terminal hydroxyl polymer PLMD was then reacted with succinic anhydride to form the terminal carboxyl functional polymer HOOC-PLMD-COOH. Finally, PEI was grafted onto HOOC-PLMD-COOH through the amidation reaction, which was activated by NHS and EDC. The structures of intermediate products of the three steps were characterized by ^1H NMR analysis (Fig. 1b–d), where the signal at 2.73 ppm was assigned to the terminal group ($COCH_2CH_2COOH$ in HOOC-PLMD-COOH) and the broad peak at 2.65 ppm (CH_2CH_2 in PEI) indicated the successful connection of PEI and PLMD.

Furthermore, the molecular weight and PDI of mPEG-*b*-PLMD, PLMD and PEI-*b*-PLMD-*b*-PEI were determined by means of GPC. All of the three polymers exhibited monomodal molecular weight distribution as shown in Fig. 2. The molecular weight of the mPEG-*b*-PLMD copolymer estimated by GPC measurements was close to the value calculated by ^1H NMR

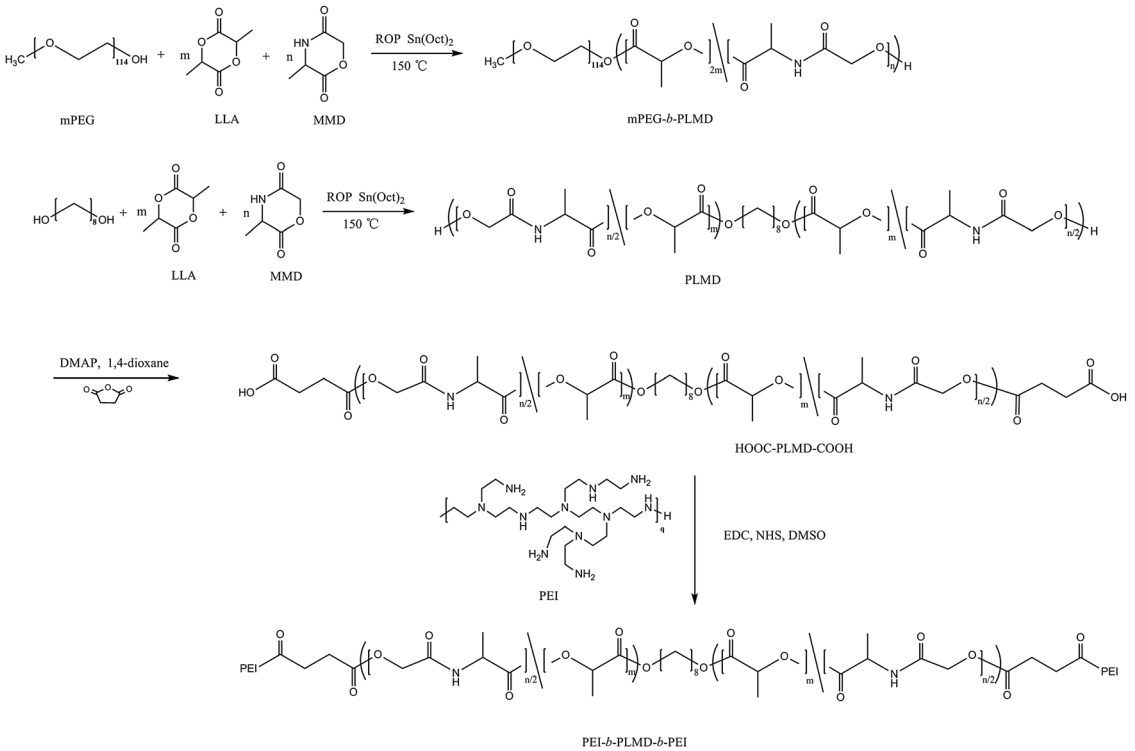

Scheme 2 Synthesis of block copolymers of mPEG-*b*-PLMD and PEI-*b*-PLMD-*b*-PEI.

spectroscopy (Table 1). Compared with PLMD, the molecular weight and PDI of the PEI-*b*-PLMD-*b*-PEI copolymer increased, which verified the successful combination of PEI and PLMD.

3.2. Zeta potential and hydrodynamic diameter of complex micelles and micelles/pDNA complexes

The co-assembly of two kinds of block copolymers, *i.e.*, mPEG-*b*-PLMD and PEI-*b*-PLMD-*b*-PEI, in aqueous solution would result in complex micelles with a hydrophobic PLMD core and a mixed hydrophilic mPEG/PEI shell. The same hydrophobic PLMD blocks in these two block copolymers were beneficial for forming the stable core of complex micelles, which can link several hydrophilic mPEG and PEI blocks as shell. In order to condense anionic pDNA for gene delivery, the micelles must contain enough cationic PEI chains. Here, we prepared four kinds of complex micelles with mass ratios (mPEG-*b*-PLMD/PEI-*b*-PLMD-*b*-PEI) of 3/1, 2/2, 1/3, and 0/4, respectively.

Using DLS, the hydrodynamic diameter (D_h) and zeta potential of these complex micelles and micelles/pDNA complexes were determined. As shown in Fig. 3, the D_h values of the four complex micelles were 147.4 nm, 135.7 nm, 140.5 nm and 88.9 nm, respectively. For the complex micelles of mPEG-*b*-PLMD/PEI-*b*-PLMD-*b*-PEI with mass ratios of 3/1 and 2/2, after condensing with pDNA, the D_h values of micelles/pDNA complexes were slightly reduced. On the other hand, an opposite trend was observed for the complex micelles of mPEG-*b*-PLMD/PEI-*b*-PLMD-*b*-PEI with mass ratios of 1/3 and 0/4, namely, the D_h values of micelles/pDNA complexes were increased after loading pDNA. When the cationic PEI chains were compressed with anionic pDNA, the PEI block in the mixed shell collapsed together with pDNA onto the PLMD core. When there were more mPEG blocks in the mixed shell (mPEG-*b*-PLMD/PEI-*b*-PLMD-*b*-PEI = 3/1 and 2/2), the collapse of PEI blocks could lead to curling of mPEG chains, which might lead to smaller size of micelles compared to micelles with no pDNA loading. When there were less mPEG blocks in the mixed shell, after the collapse of PEI, the micelles/pDNA complexes were unstable and resulted in slight aggregation. The aggregation of micelles/pDNA complexes was also observed in many polyelectrolyte colloid systems in previous studies.[53–55]

Usually, unlike the negative pDNA, gene carriers with a positive surface charge are easier to bind to the cell membrane and to achieve endocytosis. The surface charge of complex micelles and micelles/pDNA complexes was estimated by DLS. Fig. 4 shows the zeta potential of these micelles. Before condensing pEGFP-ZNF580, the zeta potential of complex micelles was positive because of the cationic PEI in the mixed shell. With decreasing content of mPEG in micelles, such as when the mass ratio of mPEG-*b*-PLMD/PEI-*b*-PLMD-*b*-PEI was decreased from 3/1 to 0/4, the zeta potential of micelles increased from +3.26 mV to +21.6 mV. The mPEG was able to shield the positive charges of PEI. But this shield effect decreased along with decreasing content of mPEG, thus resulting in high zeta potential of micelles with low mPEG content. When the ratio turned to 0/4, the micelles did not have any PEG in the shell, and showed highest zeta potential of +21.6 mV. It could be also observed that in the same group, the zeta potential increased with increasing N/P molar ratios

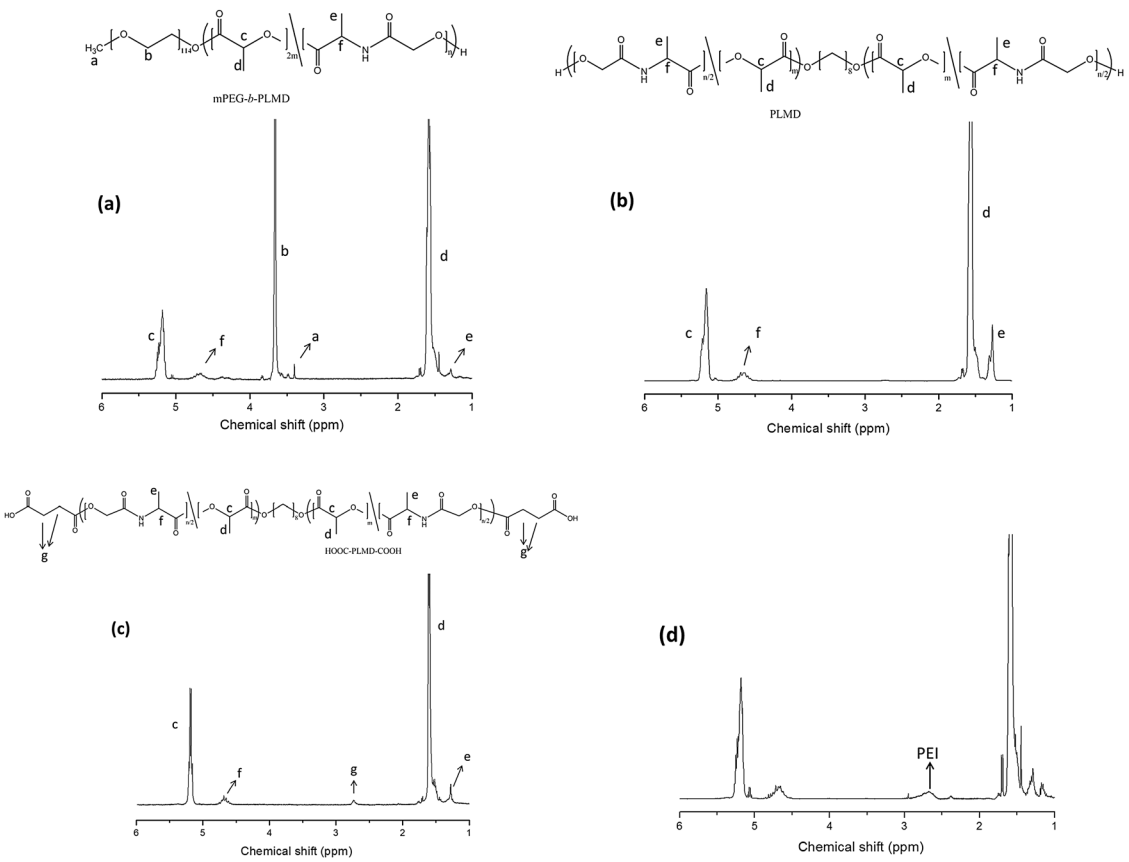

Fig. 1 ^{1}H NMR spectra of polymer mPEG-*b*-PLMD (a), PLMD (b), HOOC-PLMD-COOH (c) and PEI-*b*-PLMD-*b*-PEI (d).

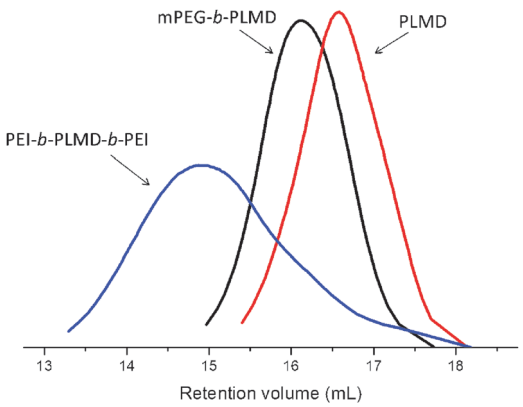

Fig. 2 GPC traces of mPEG-*b*-PLMD, PLMD and PEI-*b*-PLMD-*b*-PEI.

Table 1 Characterization of block copolymers of mPEG-*b*-PLMD and PEI-*b*-PLMD-*b*-PEI

Polymer ID	F_{LLA}[a] (%)	M_n[b]	M_n[c]	M_w[c]	PDI[c]
mPEG-*b*-PLMD	84.2	15 100	13 200	14 300	1.087
PLMD	79.6	—	10 200	11 100	1.090
PEI-*b*-PLMD-*b*-PEI	79.1	—	20 800	28 200	1.356

[a] Weight content of LLA in the PLMD block, calculated from ^{1}H NMR spectroscopy. [b] Calculated according to ^{1}H NMR. [c] Determined by means of GPC using DMF as eluent and polystyrene standards for calibration.

(Fig. 4). When the mass ratio of mPEG-*b*-PLMD/PEI-*b*-PLMD-*b*-PEI was 3/1, the zeta potential of micelles/pDNA complexes changed from negative to slightly positive with N/P molar ratios increasing from 5 to 20.

3.3. Comparing the micellar inner core of PLMD with the poly(lactide-*co*-glycolide) (PLGA) core

Fig. 5 shows the angular dependence of the translational diffusion coefficient (D_t) of mPEG-*b*-PLGA micelles and mPEG-*b*-PLMD micelles with the scattering angle ranging from 45° to 135°, respectively. It was evident that the D_t values of both kinds of micelles had no obvious dependence on q^2, which suggested that these micelles were spherical.[56] Extrapolation of the fit lines in Fig. 5 to $q^2 = 0$ yields D_t^0. Thus, the hydrodynamic radii R_h of the micelles can be calculated by the Stokes–Einstein equation.[56,57] The radii of gyration (R_g) of the two kinds of micelles were obtained from SLS at 25 °C. R_g, R_h and R_g/R_h of mPEG-*b*-PLGA micelles and mPEG-*b*-PLMD micelles are summarized in Table 2. It is well-known that the R_g/R_h value can reveal the morphology of a particle in dilute solution.[58] The R_g/R_h of mPEG-*b*-PLGA micelles was larger than that of mPEG-*b*-PLMD micelles, which indicated that the inner core of micelles composed of PLMD was more compact than that of micelles composed of PLGA. Compared with PLGA, the intermolecular hydrogen bonding inside the PLMD core could result in high

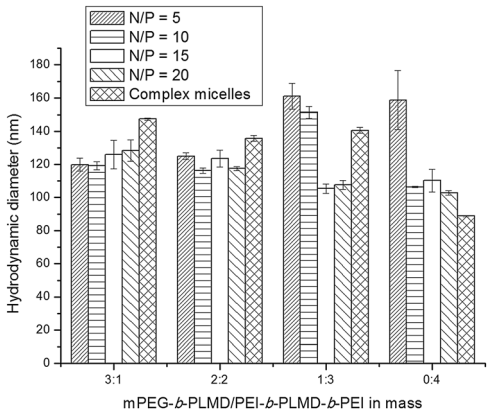

Fig. 3 Hydrodynamic diameters (D_h) of complex micelles and micelles/pDNA complexes with N/P molar ratios increasing from 5 to 20 measured by DLS.

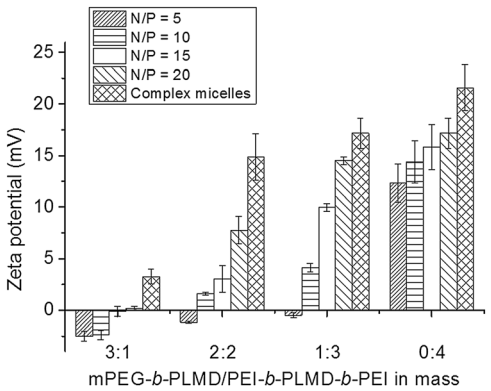

Fig. 4 Zeta potential of complex micelles and micelles/pDNA complexes with N/P molar ratios increasing from 5 to 20.

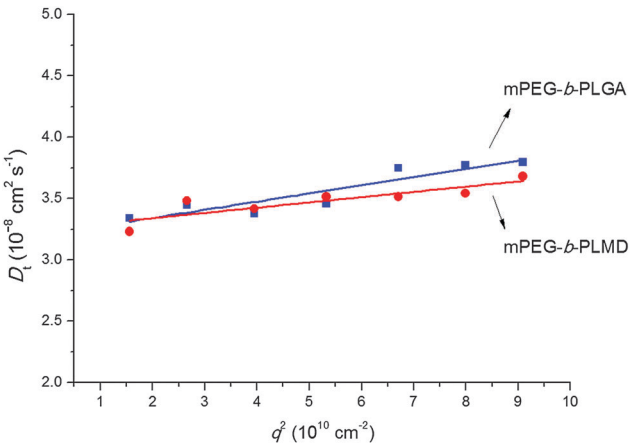

Fig. 5 Angular dependence of D_t of mPEG-*b*-PLGA micelles and mPEG-*b*-PLMD micelles, where the polymer concentration was 0.50 mg mL^{-1} in all cases. All of the SLS measurements were performed at 25 °C.

compactness of the micellar core, and micelles assembled from mPEG-*b*-PLMD would be more stable than those assembled from mPEG-*b*-PLGA.

Table 2 R_g, R_h and R_g/R_h of mPEG-*b*-PLGA micelles and mPEG-*b*-PLMD micelles at 25 °C

Micelles	R_g (nm)	R_h (nm)	R_g/R_h
mPEG-*b*-PLGA	74.9	76.1	0.984
mPEG-*b*-PLMD	67.2	75.1	0.895

3.4. pDNA complexation and condensation

In order to determine the ability of complex micelles to condense pDNA, agarose gel electrophoresis assays were performed. The results are shown in Fig. 6. The complex micelles with different mPEG-*b*-PLMD/PEI-*b*-PLMD-*b*-PEI ratios (3/1, 2/2, 1/3 and 0/4) could achieve complete retardation of pDNA (indicating complete pDNA complexation) at N/P = 5, 5, 3 and 3, respectively. When the content of mPEG was high in the mixed shell, pDNA could not be condensed completely at low N/P molar ratios. This indicated that the mPEG block in the mixed shell could hinder the interaction of micelles and pDNA. Enhanced pDNA condensation could be achieved by increasing the content of the PEI block in the mixed shell.

3.5. *In vitro* cytotoxicity of complex micelles and micelles/pDNA complexes

The cytotoxicity of complex micelles and micelles/pDNA complexes was investigated in EA.hy926 cells by MTT assays. PEI 10 kDa was used as a control. The concentrations of complex micelles and micelles/pDNA complexes ranged from 10 to 120 mg L^{-1}. The relative viabilities of cells treated with the complexes were measured after 24 h by MTT assay. The results showed that all complex micelles and micelles/pDNA complexes were practically less toxic to EA.hy926 cells than PEI 10 kDa with different concentrations of micelles at a N/P molar ratio of 15 (Fig. 7). In particular, the cytotoxicity of complex micelles generally reduced after loading pDNA, which was conducive to the following transfection experiments. Notably, it was observed that with decreasing content of the mPEG block in the mixed shell (the mass ratio of mPEG-*b*-PLMD/PEI-*b*-PLMD-*b*-PEI changed from 3/1 to 0/4), the cell viability of EA.hy926 cells with complex micelles and micelles/pDNA complexes decreased.

3.6. *In vitro* gene transfection of micelles/pDNA complexes

The existence of mPEG blocks around the micelles can shield the surface charge of micelles so that they are beneficial for reducing the cytotoxicity of these gene carriers. In the following transfection experiments, we aim to investigate the relationship between the mass ratios of mPEG-*b*-PLMD/PEI-*b*-PLMD-*b*-PEI and the transfection efficiency of micelles/pDNA complexes. *In vitro* gene transfection activity of micelles/pDNA complexes was evaluated in EA.hy926 cells at a N/P molar ratio of 15 with the concentration of micelle solutions being 30 μg mL^{-1}. The transfection efficiency of micelles/pDNA complexes was visualized by the observation of EGFP positive cells using a fluorescence microscope (Fig. 8). All the four kinds of micelles showed good transfection activity after 12 h, and the transfection

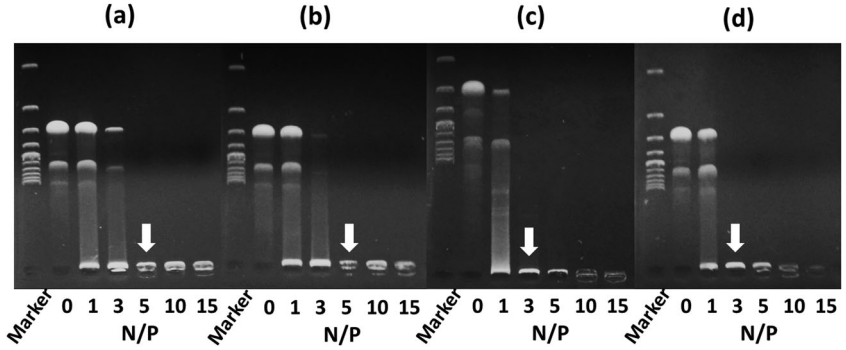

Fig. 6 Agarose gel electrophoresis of micelles/pDNA complexes at various N/P ratios (Marker, 0, 1, 3, 5, 10 and 15). (a) Complex micelles with mPEG-*b*-PLMD/PEI-*b*-PLMD-*b*-PEI = 3/1; (b) complex micelles with mPEG-*b*-PLMD/PEI-*b*-PLMD-*b*-PEI = 2/2; (c) complex micelles with mPEG-*b*-PLMD/PEI-*b*-PLMD-*b*-PEI = 1/3; (d) complex micelles with mPEG-*b*-PLMD/PEI-*b*-PLMD-*b*-PEI = 0/4.

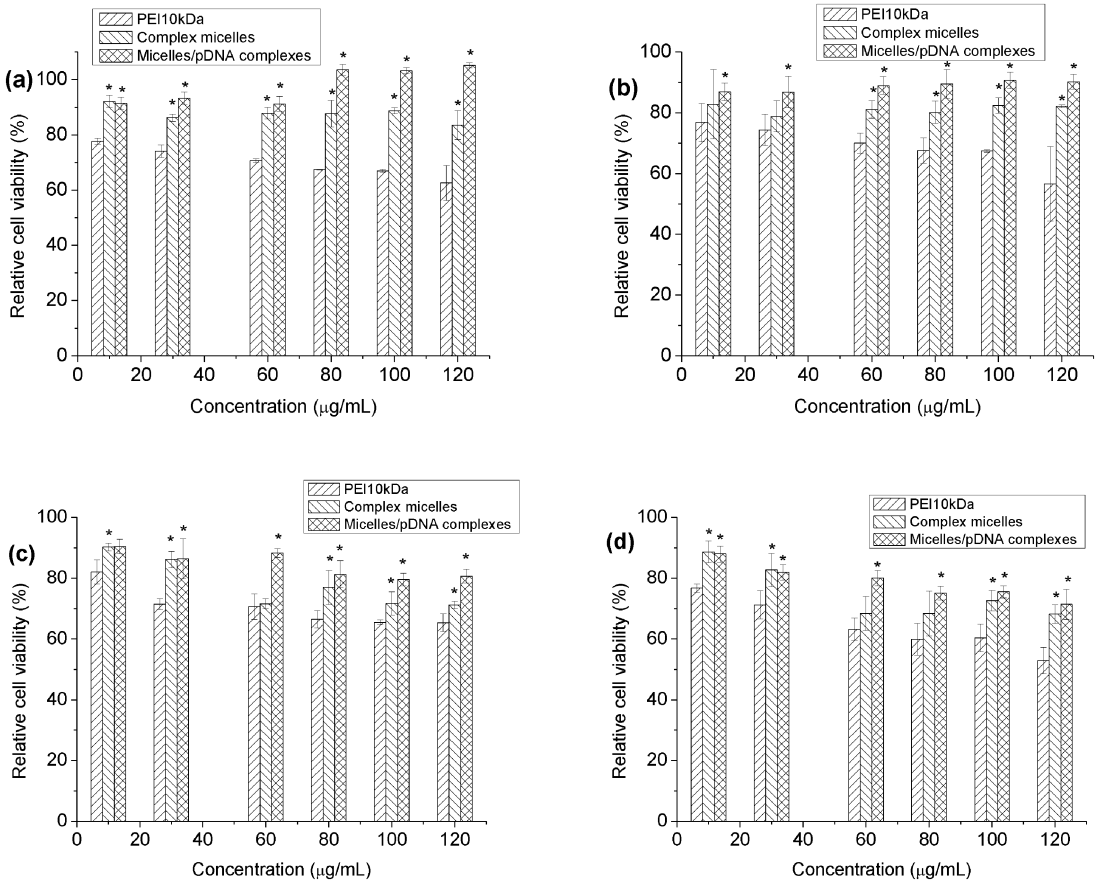

Fig. 7 Relative cell viability of EA.hy926 cells with different concentrations of micelles at a N/P molar ratio of 15. Cells treated with PEI 10 kDa served as the control group. (a) Cells treated with complex micelles and micelles/pDNA complexes with mPEG-*b*-PLMD/PEI-*b*-PLMD-*b*-PEI = 3/1; (b) cells treated with complex micelles and micelles/pDNA complexes with mPEG-*b*-PLMD/PEI-*b*-PLMD-*b*-PEI = 2/2; (c) cells treated with complex micelles and micelles/pDNA complexes with mPEG-*b*-PLMD/PEI-*b*-PLMD-*b*-PEI = 1/3; (d) cells treated with complex micelles and micelles/pDNA complexes with mPEG-*b*-PLMD/PEI-*b*-PLMD-*b*-PEI = 0/4. ($\bar{x} \pm$ SD, n = 3, * statistically different from the PEI 10 kDa group ($p < 0.05$).)

efficiency was enhanced after 24 h. The trend was clear: with increasing content of the PEI block in the mixed shell (the mass ratio of mPEG-*b*-PLMD/PEI-*b*-PLMD-*b*-PEI decreased from 3/1 to 0/4), the transfection efficiency of micelles/pDNA complexes increased. The co-assembly of PEI with mPEG could shield the surface charge of micelles, reduce the cytotoxicity of these gene carriers and meanwhile remarkably diminish transfection efficiency in EA.hy926 cells.

3.7. Western blot assay

The Western blot assay was used to confirm the expression of the ZNF580 gene in EA.hy926 cells. As shown in Fig. 9, the

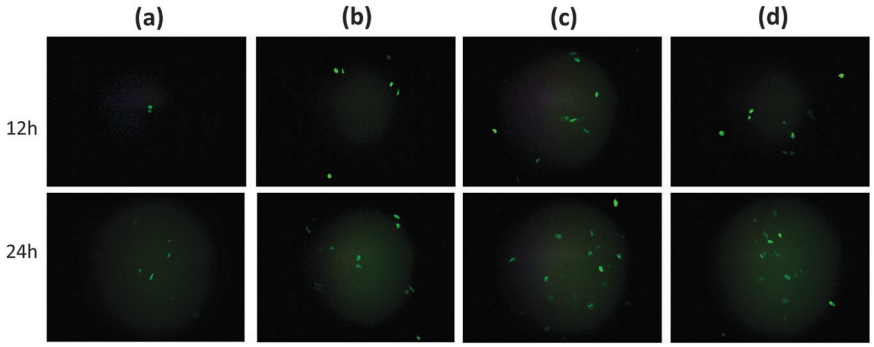

Fig. 8 Fluorescence images of EA.hy926 cells transfected by micelles/pDNA complexes at the N/P molar ratio of 15 and time intervals of 12 h and 24 h. (a) Cells treated with micelles/pDNA complexes with mPEG-*b*-PLMD/PEI-*b*-PLMD-*b*-PEI = 3/1; (b) cells treated with micelles/pDNA complexes with mPEG-*b*-PLMD/PEI-*b*-PLMD-*b*-PEI = 2/2; (c) cells treated with micelles/pDNA complexes with mPEG-*b*-PLMD/PEI-*b*-PLMD-*b*-PEI = 1/3; (d) cells treated with micelles/pDNA complexes with mPEG-*b*-PLMD/PEI-*b*-PLMD-*b*-PEI = 0/4.

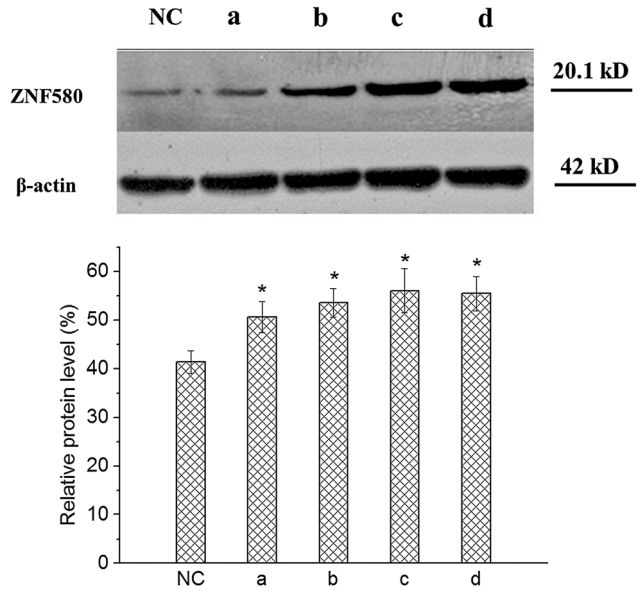

Fig. 9 Western blot analysis for ZNF580 protein expression in EA.hy926 cells transfected by micelles/pDNA complexes; cells without treatment with micelles/pDNA complexes served as the NC group. (a) Cells treated with micelles/pDNA complexes with mPEG-*b*-PLMD/PEI-*b*-PLMD-*b*-PEI = 3/1; (b) cells treated with micelles/pDNA complexes with mPEG-*b*-PLMD/PEI-*b*-PLMD-*b*-PEI = 2/2; (c) cells treated with micelles/pDNA complexes with mPEG-*b*-PLMD/PEI-*b*-PLMD-*b*-PEI = 1/3; (d) cells treated with micelles/pDNA complexes with mPEG-*b*-PLMD/PEI-*b*-PLMD-*b*-PEI = 0/4. ($\bar{x} \pm$ SD, n = 3, * statistically different from the NC group ($p < 0.05$).)

Western blot analysis indicated that after 48 h of transfection, the ZNF580 protein expression was clearly visible at the N/P molar ratio of 15 for the micelles/pDNA complexes. The degree of ZNF580 protein expression of micelles/pDNA complexes was higher than the negative control group (NC). Different micelles exhibited effective up-regulation, when the ratios of mPEG-*b*-PLMD/PEI-*b*-PLMD-*b*-PEI changed from 3/1 to 0/4. This result was consistent with the results of transfection efficiency. High gene transfection efficiency of the micelles/pDNA complexes is beneficial for high ZNF580 protein expression.

3.8. Wound healing assay

Results from wound healing assay are shown in Fig. 10. Compared with the NC group, all of the four kinds of micelles/pDNA complexes obviously promoted the migration of EA.hy926 cells. The migration rate of transfected cells increased with the mass ratio of mPEG-*b*-PLMD/PEI-*b*-PLMD-*b*-PEI changing from 3/1 to 0/4. After 12 h of scratch formation, the migration area percentage of the NC group was only 32.4 ± 4.3%, while cells treated with micelles/pDNA complexes prepared from PEI-*b*-PLMD-*b*-PEI (the mass ratio of mPEG-*b*-PLMD/PEI-*b*-PLMD-*b*-PEI was 0/4) reached a high migration area percentage (almost 100%). These results suggested that the complex micelles condensed with pDNA could enhance the migration of EA.hy926 cells. The high content of the PEI block in the mixed shell of complex micelles is beneficial for high transfection efficiency as well as high cell migration.

4. Discussion

Rapid endothelialization has been proposed to solve in-stent restenosis after the stent implantation in the treatment of occluded coronary arteries.[59,60] For the realization of rapid endothelialization in artificial vascular grafts, gene therapy as a potential strategy has been highlighted recently.[2] Apart from viral carriers, nonviral gene delivery systems, especially cationic polymer-based gene delivery systems, have attracted increasing attention due to safety concerns and easy modification of their structures.[10,61] Many research studies of nonviral gene delivery carriers focus on reducing the cytotoxicity and enhancing the transfection efficiency of gene carriers simultaneously. In parallel with the efforts to synthesize special polymers through modern polymerization techniques, the approach of co-assembly of different functional block copolymers into complex polymeric micelles offers a convenient preparation process for multifunctional gene carriers.[62–64] This strategy is beneficial for tuning the outer surface of complex micelles.

In this study, the co-assembly technology was applied to tailor the transfection efficiency and cytotoxicity of gene

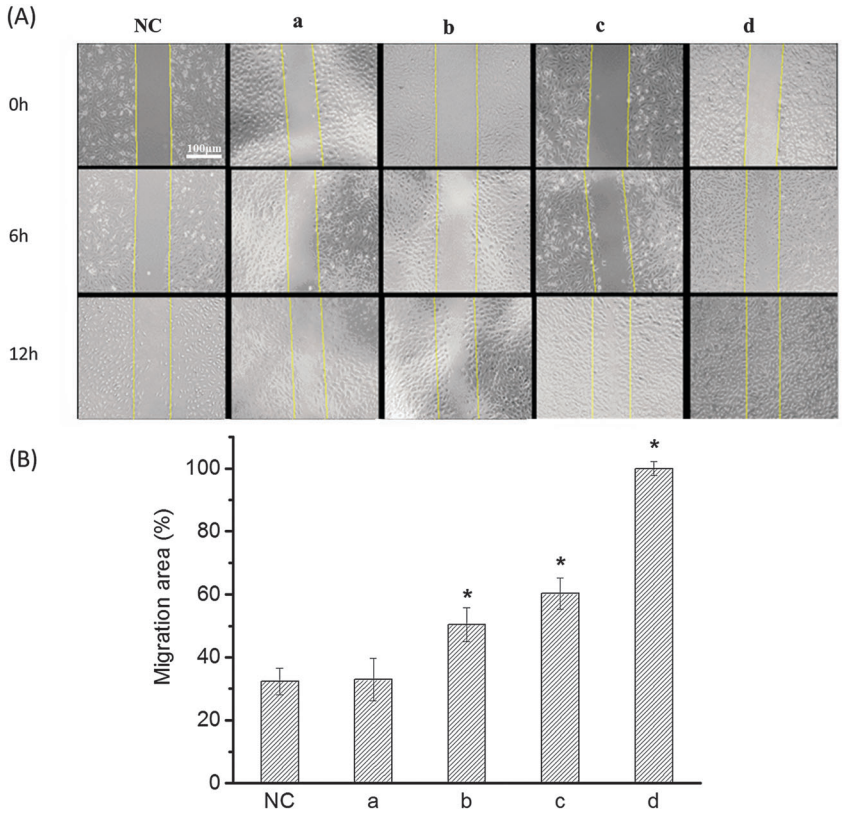

Fig. 10 (A) Cell migration determined by wound healing assay at different time points. (B) Migration area after 12 h calculated by using Image-Pro Plus (6.0). Cells without treatment with micelles/pDNA complexes served as the NC group. (a) Cells treated with micelles/pDNA complexes with mPEG-*b*-PLMD/PEI-*b*-PLMD-*b*-PEI = 3/1; (b) cells treated with micelles/pDNA complexes with mPEG-*b*-PLMD/PEI-*b*-PLMD-*b*-PEI = 2/2; (c) cells treated with micelles/pDNA complexes with mPEG-*b*-PLMD/PEI-*b*-PLMD-*b*-PEI = 1/3; (d) cells treated with micelles/pDNA complexes with mPEG-*b*-PLMD/PEI-*b*-PLMD-*b*-PEI = 0/4. ($\bar{x} \pm$ SD, n = 3, * statistically different from the NC group ($p < 0.05$).)

carriers *via* predefining the amount of mPEG and PEI on the micellar surface. Hydrophobic PLMD segments formed the inner core to increase the biodegradability of the polymeric micelles. In previous research, we have successfully prepared complex micelles consisting of a biodegradable PLGA core and a mixed PEG/PEI shell.[65] The results of DLS and SLS showed that the R_g/R_h of mPEG-*b*-PLGA micelles was larger than that of mPEG-*b*-PLMD micelles, which indicated that the inner core of micelles composed of PLMD was more compact than that of micelles composed of PLGA. The existence of intermolecular hydrogen bonding in the micellar core formed by PLMD chains is beneficial for forming highly stable micelles than the PLGA core.

According to the results of zeta potential, the nano-sized micelles co-assembled from mPEG-*b*-PLMD and PEI-*b*-PLMD-*b*-PEI possessed a positive surface charge due to the polycationic PEI which directly led to high cytotoxicity evaluated in EA.hy926 cells by MTT assays. As previously reported,[25,66] the cytotoxicity of polycationic micelles may presumably be caused by aggregation of huge clusters of cationic polymers on the outer cell membrane, thereby inducing necrosis. When cationic PEI-*b*-PLMD-*b*-PEI was co-assembled with electroneutral mPEG-*b*-PLMD, the reduction of micellar cytotoxicity could be a function of the content of mPEG in the complex micellar shell. Thus the cell viability presented an increasing trend when the mPEG-*b*-PLMD/PEI-*b*-PLMD-*b*-PEI mass ratio increased from 0/4 to 3/1. But the high positive charge of complex micelles was favorable for the high condensation ability of negative pDNA *via* electrostatic interactions.

To investigate the gene transfection efficiency of micelles/pDNA complexes with different mPEG-*b*-PLMD/PEI-*b*-PLMD-*b*-PEI mass ratios, we transfected EA.hy926 cells with pDNA at a N/P molar ratio of 15 with the concentration of micelle solutions being 30 μg mL^{-1} *in vitro*. Unlike the results of MTT assay, the transfection efficiency showed an increasing tendency when the mPEG-*b*-PLMD/PEI-*b*-PLMD-*b*-PEI mass ratio decreased from 3/1 to 0/4. The high content of PEI chains in the mixed shell of micelles would lead to high transfection efficiency, and the micelles with a mPEG-*b*-PLMD/PEI-*b*-PLMD-*b*-PEI mass ratio of 0/4 were the most effective gene carriers. Although the presence of PEI chains significantly caused high cytotoxicity of micelles/pDNA complexes, the transfection efficiency of micelles increased at the same time. The results of Western blot assay at 48 h after transfection showed a clearly noticeable rise in protein levels with increasing content of PEI chains in the mixed shell, which was consistent with the results of transfection experiments. The increase in the content of PEI chains in the micelles improved the transfection of pZNF580 into EA.hy926 cells and simultaneously raised the relative ZNF580 protein levels.

The migratory capability of cells was measured by wound healing assay. The enhanced migration was dependent on the mass ratio of mPEG-*b*-PLMD/PEI-*b*-PLMD-*b*-PEI of the micelles. Cells treated by micelles/pDNA complexes assembled from PEI-*b*-PLMD-*b*-PEI (the mass ratio of mPEG-*b*-PLMD/PEI-*b*-PLMD-*b*-PEI was 0/4) migrated and covered the wound area with a relatively high migration area percentage (almost 100%) due to the high transfection efficiency of the pZNF580 gene to improve the migration of ECs. These results suggested that these ZNF580 gene plasmid-loaded micelles are beneficial for the transfection of ECs.

5. Conclusions

In this study, we developed a novel gene carrier to adjust the cytotoxicity and the transfection efficiency. The delivery of the ZNF580 gene plasmid into EA.hy926 cells was successfully carried out by the co-assembled complex micelles with a hydrophobic PLMD core and a mixed mPEG/PEI shell. The small hydrodynamic size and positive zeta potential of micelles/pDNA complexes indicated that they were feasible for use in cellular uptake and gene transfection. The cytotoxicity and transfection of the ECs could be tuned by changing the ratio of mPEG to PEI in the mixed shell. Moreover, Western blot analysis confirmed that the micelles/pDNA complexes could enhance the expression of ZNF580 in cells, and the expression could be effectively up-regulated by increasing the content of the PEI block in the mixed shell of complex micelles. Finally, wound healing assay demonstrated the enhanced migration activity of ECs by micelles/pDNA complexes depending on increasing the amount of the PEI block in the mixed shell. These results indicated that the co-assembled complex micelles could be promising gene carriers with tunable gene transfection efficiency and cytotoxicity.

Acknowledgements

This project was supported by the National Natural Science Foundation of China, China (Grant No. 31370969), the International Cooperation from Ministry of Science and Technology of China, China (Grant No. 2013DFG52040), and the Program of Introducing Talents of Discipline to Universities of China, China (No. B06006).

References

1 X. K. Ren, Y. K. Feng, J. T. Guo, H. X. Wang, Q. Li, J. Yang, X. F. Hao, J. Lv, N. Ma and W. Z. Li, *Chem. Soc. Rev.*, 2015, **44**, 5680–5742.
2 Y. W. Won, M. Lee, H. A. Kim, K. Nam, D. A. Bull and S. W. Kim, *Mol. Pharmaceutics*, 2013, **10**, 3676–3683.
3 G. Zuber, M. Dontenwill and J. P. Behr, *Mol. Pharmaceutics*, 2009, **6**, 1544–1552.
4 J. Yang, Y. Zeng, C. Zhang, Y. X. Chen, Z. Yang, Y. Li, X. Leng, D. Kong, X. Q. Wei and H. F. Sun, *Biomaterials*, 2013, **34**, 1635–1643.
5 H. Y. Sun, S. P. Wei, R. C. Xu, P. X. Xu and W. C. Zhang, *Biochem. Biophys. Res. Commun.*, 2010, **395**, 361–366.
6 C. C. Shi, F. L. Yao, Q. Li, M. Khan, X. K. Ren, Y. K. Feng, J. W. Huang and W. C. Zhang, *Biomaterials*, 2014, **35**, 7133–7145.
7 C. C. Shi, F. L. Yao, J. W. Huang, G. L. Han, Q. Li, M. Khan, Y. K. Feng and W. C. Zhang, *J. Mater. Chem. B*, 2014, **2**, 1825–1837.
8 L. Yu, Y. K. Feng, Q. Li, X. F. Hao, W. Liu, W. Zhou, C. C. Shi, X. K. Ren and W. C. Zhang, *React. Funct. Polym.*, 2015, **91–92**, 19–27.
9 M. A. Mintzer and E. E. Simanek, *Chem. Rev.*, 2009, **109**, 259–302.
10 M. Neu, D. Fischer and T. Kissel, *J. Gene Med.*, 2005, **7**, 992–1009.
11 H. Q. Song, X. B. Dou, R. Q. Li, B. R. Yu, N. N. Zhao and F. J. Xu, *Acta Biomater.*, 2015, **12**, 156–165.
12 H. Hu, H. Q. Song, B. R. Yu, Q. Cai, Y. Zhu and F. J. Xu, *Polym. Chem.*, 2015, **6**, 2466–2477.
13 X. B. Dou, Y. Hu, N. N. Zhao and F. J. Xu, *Biomaterials*, 2014, **35**, 3015–3026.
14 R. Q. Li, Y. L. Niu, N. N. Zhao, B. R. Yu, C. Mao and F. J. Xu, *ACS Appl. Mater. Interfaces*, 2014, **6**, 3969–3978.
15 P. Yan, R. R. Wang, N. N. Zhao, H. Zhao, D. F. Chen and F. J. Xu, *Nanoscale*, 2015, **7**, 5281–5291.
16 Y. He, Y. Nie, G. Cheng, L. Xie, Y. Shen and Z. Gu, *Adv. Mater.*, 2014, **26**, 1534–1540.
17 J. Luo, C. Li, J. Chen, G. Wang, R. Gao and Z. Gu, *Int. J. Nanomed.*, 2015, **10**, 1667–1678.
18 L. Pu, Y. Geng, S. Liu, J. Chen, K. Luo, G. Wang and Z. Gu, *ACS Appl. Mater. Interfaces*, 2014, **6**, 15344–15351.
19 J. Chang, X. Xu, H. Li, Y. Jian, G. Wang, B. He and Z. Gu, *Adv. Funct. Mater.*, 2013, **23**, 2691–2699.
20 S. Browne and A. Pandit, *J. Mater. Chem. B*, 2014, **2**, 6692–6707.
21 A. Mathew, W. X. Wang and A. Pandit, *Pharm. Nanotechnol.*, 2014, **2**, 35–41.
22 H. Tian, Z. Guo, L. Lin, Z. Jiao, J. Chen, S. Gao, X. Zhu and X. Chen, *J. Controlled Release*, 2014, **174**, 117–125.
23 S. Y. Wong, J. M. Pelet and D. Putnam, *Prog. Polym. Sci.*, 2007, **32**, 799–837.
24 D. Fischer, Y. X. Li, B. Ahlemeyer, J. Krieglstein and T. Kissel, *Biomaterials*, 2003, **24**, 1121–1131.
25 D. Fischer, T. Bieber, Y. Li, H. P. Elsasser and T. Kissel, *Pharm. Res.*, 1999, **16**, 1273–1279.
26 V. C. F. Mosqueira, P. Legrand, R. Gref, B. Heurtault, M. Appel and G. Barratt, *J. Drug Targeting*, 1999, **7**, 65–78.
27 P. Wang, K. L. Tan and E. T. Kang, *J. Biomater. Sci., Polym. Ed.*, 2000, **11**, 169–186.
28 J. H. Lee, H. B. Lee and J. D. Andrade, *Prog. Polym. Sci.*, 1995, **20**, 1043–1079.
29 S. I. Jeon, J. H. Lee, J. D. Andrade and P. G. De Gennes, *J. Colloid Interface Sci.*, 1991, **142**, 149–158.

30 T. K. Endres, M. Beck-Broichsitter, O. Samsonova, T. Renette and T. Kissel, *Biomaterials*, 2011, **32**, 7721–7731.
31 M. Ogris, S. Brunner, S. Schuller, R. Kircheis and E. Wagner, *Gene Ther.*, 1999, **6**, 595–605.
32 P. Erbacher, T. Bettinger, P. Belguise-Valladier, S. M. Zou, J. L. Coll, J. P. Behr and J. S. Remy, *J. Gene Med.*, 1999, **1**, 210–222.
33 H. Cabral, N. Nishiyama and K. Kataoka, *Acc. Chem. Res.*, 2011, **44**, 999–1008.
34 H. Yuan, K. Luo, Y. Lai, Y. Pu, B. He, G. Wang, Y. Wu and Z. Gu, *Mol. Pharmaceutics*, 2010, **7**, 953–962.
35 H. X. Wang, Y. K. Feng, J. Yang, J. T. Guo and W. C. Zhang, *J. Mater. Chem. B*, 2015, **3**, 3379–3391.
36 Q. Li, C. C. Shi, W. C. Zhang, M. Behl, A. Lendlein and Y. K. Feng, *Adv. Healthcare Mater.*, 2015, **4**, 1225–1235.
37 Z. Zhang, R. Ma and L. Shi, *Acc. Chem. Res.*, 2014, **47**, 1426–1437.
38 Y. Zhong, W. Yang, H. Sun, R. Cheng, F. Meng, C. Deng and Z. Zhong, *Biomacromolecules*, 2013, **14**, 3723–3730.
39 F. Gu, L. Zhang, B. A. Teply, N. Mann, A. Wang, A. F. Radovic-Moreno, R. Langer and O. C. Farokhzad, *Proc. Natl. Acad. Sci. U. S. A.*, 2008, **105**, 2586–2591.
40 Y. K. Feng, J. Lu, M. Behl and A. Lendlein, *Macromol. Biosci.*, 2010, **10**, 1008–1021.
41 Y. K. Feng, M. Behl, S. Kelch and A. Lendlein, *Macromol. Biosci.*, 2009, **9**, 45–54.
42 Y. K. Feng, D. Klee and H. Hocker, *J. Polym. Sci., Part A: Polym. Chem.*, 2005, **43**, 3030–3039.
43 J. Lv, L. Zhang, M. Khan, X. K. Ren, J. T. Guo and Y. K. Feng, *React. Funct. Polym.*, 2014, **82**, 89–97.
44 M. Deshmukh, Y. Singh, S. Gunaseelan, D. Gao, S. Stein and P. J. Sinko, *Biomaterials*, 2010, **31**, 6675–6684.
45 S. Mallakpour, S. Soltanian and M. R. Sabzalian, *Colloid Polym. Sci.*, 2011, **289**, 93–100.
46 Y. Liu, O. Samsonova, B. Sproat, O. Merkel and T. Kissel, *J. Controlled Release*, 2011, **153**, 262–268.
47 T. Endres, M. Zheng, A. Kilic, A. Turowska, M. Beck-Broichsitter, H. Renz, O. M. Merkel and T. Kissel, *Mol. Pharmaceutics*, 2014, **11**, 1273–1281.
48 H. R. Kricheldorf and K. Hauser, *Macromol. Chem. Phys.*, 2001, **202**, 1219–1226.
49 R. Yang, S. Zhang, D. Kong, X. Gao, Y. Zhao and Z. Wang, *Pharm. Res.*, 2012, **29**, 3512–3525.
50 D. L. Ren, H. K. Wang, J. Q. Liu, M. H. Zhang and W. C. Zhang, *Mol. Cell. Biochem.*, 2012, **359**, 183–191.
51 M. Zubair, A. Ekholm, H. Nybom, S. Renvert, C. Widen and K. Rumpunen, *J. Ethnopharmacol.*, 2012, **141**, 825–830.
52 W. C. Hung and H. C. Chang, *J. Agric. Food Chem.*, 2009, **57**, 76–82.
53 Y. L. Wang, K. Kimura, P. L. Dubin and W. Jaeger, *Macromolecules*, 2000, **33**, 3324–3331.
54 F. Bordi, C. Cametti, S. Sennato and M. Diociaiuti, *Biophys. J.*, 2006, **91**, 1513–1520.
55 V. Milkova, K. Kamburova, I. Petkanchin and T. Radeva, *Langmuir*, 2008, **24**, 9495–9499.
56 W. Q. Zhang, L. Q. Shi, Y. L. An, L. C. Gao and B. L. He, *J. Phys. Chem. B*, 2004, **108**, 200–204.
57 R. Ma, B. Wang, X. Liu, Y. An, Y. Li, Z. He and L. Shi, *Langmuir*, 2007, **23**, 7498–7504.
58 C. Wu, M. Siddiq and K. F. Woo, *Macromolecules*, 1995, **28**, 4914–4919.
59 Y. Wei, Y. Ji, L. L. Xiao, Q. K. Lin, J. P. Xu, K. F. Ren and J. Ji, *Biomaterials*, 2013, **34**, 2588–2599.
60 T. C. Woods and A. R. Marks, *Annu. Rev. Med.*, 2004, **55**, 169–178.
61 X. F. Hao, Q. Li, J. Lv, L. Yu, X. K. Ren, L. Zhang, Y. K. Feng and W. C. Zhang, *ACS Appl. Mater. Interfaces*, 2015, **7**, 12128–12140.
62 F. J. Xu and W. T. Yang, *Prog. Polym. Sci.*, 2011, **36**, 1099–1131.
63 J. J. Nie, X. B. Dou, H. Hu, B. G. Yu, D. F. Chen, R. X. Wang and F. J. Xu, *ACS Appl. Mater. Interfaces*, 2015, **7**, 553–562.
64 Y. Hua, W. Yuan, N. N. Zhao, J. Ma, W. T. Yang and F. J. Xu, *Biomaterials*, 2013, **34**, 5411–5422.
65 J. Lv, X. F. Hao, J. Yang, Y. K. Feng, M. Behl and A. Lendlein, *Macromol. Chem. Phys.*, 2014, **215**, 2463–2472.
66 R. Kircheis, L. Wightman and E. Wagner, *Adv. Drug Delivery Rev.*, 2001, **53**, 341–358.

